ELSEVIER

Energy and Buildings 25 (1997) 149–158

ENERGY AND BUILDINGS

Preliminary survey of the solar reflectance of cool roofing materials

Paul Berdahl, Sarah E. Bretz [1]

Energy and Environment Division, Lawrence Berkeley National Laboratory, Berkeley, CA 94720, USA

Abstract

Air-conditioning energy savings and improved comfort in hot climates can be obtained with the use of roofing materials that reflect solar radiation. Available quantitative information on the solar reflectance of most roofing materials is insufficient, so it is difficult for building designers to choose cool materials. Here we report quantitative values of solar reflectance for a few types of materials and discuss which material properties, such as composition, roughness, purity, etc., affect the solar reflectance. Outdoor temperature measurements on materials in sunlight are used to illustrate the strong correlation of roof temperature with solar absorptance, and further, to demonstrate the effects of infrared emittance and convection.

Keywords: Air-conditioning energy savings; Roofing materials; Solar reflectance; Solar absorptance; Roof material properties

1. Introduction

Several studies have documented air-conditioning energy savings in buildings achieved by increasing exterior albedo, i.e., solar reflectance. Field tests in Florida resulted in cooling energy savings ranging from 10 to 43%, with the application of high albedo coatings to various roofs [1]. Reduction in utility coincident peak demand (5 to 6 p.m.) was 16–38% in the same buildings. Energy savings were significant even with well-insulated roofs. In Mississippi, cooling energy savings of 22% for the summer were achieved through the application of a high-albedo coating [2], while there was no penalty in the winter. In Sacramento, California, several buildings had cooling energy savings of 40–50% and 30–40% peak demand reductions through high-albedo roof retrofits [3].

Air-conditioning savings are achieved by reducing the temperature of the building exterior, which in turn reduces the heat flow through the building envelope. Exterior surface temperatures may be reduced by increasing the solar reflectance or the infrared emittance. A high solar reflectance reduces solar heating, and a high infrared emittance increases radiative cooling. Often, the application of a high-albedo coating to a building exterior increases the solar reflectance without appreciable change in infrared emittance. The exception is when such a coating is applied to a low emittance substrate, such as a metal roof. One of the test cases above involved both an increase in solar reflectance and infrared emittance [3]. Other studies have also discussed various aspects of the thermal performance of solar reflective coatings [4–7]. Of course, the general idea of white washing structures to reject heat has been known since antiquity.

While the emphasis of this paper is on cool roofing materials, it is important to keep in mind that the primary function of the roof is to protect the underlying structure from the weather for a long period of time, at a low cost. Environmental stresses which must be resisted include temperature cycling caused by sunlight and sudden temperature swings (e.g., due to rain), solar ultraviolet radiation, moisture penetration and condensation, wind, hail, biological growth, atmospheric pollution, freeze–thaw cycles, and stresses due to walking on the roof. The energy benefit of a cool roof will usually be a secondary consideration for the building owner, who must consider issues of appearance, fire safety, etc., as well. However, in many cases there need be no contradiction between energy conservation and roof lifetime considerations. In fact, reflective materials have the potential to extend roofing lifetimes.

The purpose of this paper is to report measured data on the solar reflectance of materials which are now, or may in the future, be used in roofs. The precise energy benefits from the control of radiation, however, depend on the performance of the complete roof structure, and indeed, on the rest of the structure. In lieu of a complete analysis, which is beyond the scope of this paper, we offer some observations about the rest

[1] Present address: Washington Office of the Lawrence Berkeley National Laboratory, 1250 Maryland Ave SW, Suite 500, Washington DC 20024.

Published by Elsevier Science S.A.
PII S0378-7788(96)01004-3

of the heat transfer problem. The use of thermal insulation beneath the roof helps to limit the flow of heat into the building. However, the temperature rise of the roof in the sun is quite significant, even for white roofs, and the roof area is large, so that the heat flow through the insulation can be quite significant. It is worth noting in this connection that the R value of insulation generally decreases at elevated temperatures [7], because the thermal conductivity of air (which gives the insulation much of its resistance) increases with increasing temperature; radiant transfer within the insulation also is more effective at higher temperature. Furthermore, non-ideal aspects of the heating ventilating and air-conditioning (HVAC) system design (e.g., air-conditioning ducts in the attic, even leaking attic ducts) can contribute to unanticipated leakage of solar heat into the building. The dominant parameters which determine the maximum roof temperatures are the solar absorptance, infrared emittance, and the convection coefficient. The convection coefficient is important: convection carries away at least as much of the absorbed solar heat as infrared re-radiation. Certain tile roofs benefit from enhanced convection due to air circulation under as well as over the tile [8]. In a similar vein, plenum ventilation can be employed, in attic or roof, to carry away some of the heat which would otherwise enter the building. Finally, we note that the use of architectural features such as parapets or screens (e.g., to hide equipment on roofs) can reduce ambient air flow near the roof surface and reduce the convection coefficient, thereby increasing roof temperatures. We are focusing on roofs, but clearly the west and east walls of buildings also present opportunities for reflective surfaces to contribute to energy conservation.

Some limited data on albedo (solar reflectance) of various building materials has been published. Taha [9] compiled data from a number of sources and presented some results from field measurements. Reagan and Acklam [10] published useful tables of measured data on the solar reflectance of common building materials, as part of a study on roof temperatures. However, the sensor for these measurements was a silicon photodiode which was sensitive only in the limited spectral range from 0.44 to 0.96 μm. Thus the actual albedo has not been accurately determined. Complete spectral data for building materials are more limited, with a notable contribution made by Parker, McIlvaine, Barkaszi, and Beal [11]. Touloukian et al. [12] present a valuable compilation of spectral information on a variety of materials, including white paints that contain titanium dioxide pigments. Thus, in some cases the solar reflectance can be computed based on published values of spectral reflectance in the relevant 0.3 to 2.5 μm spectral range.

In contrast to the limited spectral data available for opaque building materials, the situation for architectural glazing is much more satisfactory. For example, Furler et al. [13] have presented complete spectral transmittance and reflectance data for many commercial glazings for wavelengths from 0.2 μm all the way out to 45 μm.

2. Sensitivity of roof temperature to roof and environmental parameters

Roof temperature is a key parameter which essentially determines the (solar-induced) heat leakage through the roof insulation into the space below. The roof temperature itself is not highly sensitive to the details of the building construction below the roof surface because the heat transfers occurring at the outer surface are usually more vigorous than the heat transfers in the interior. This is particularly true if insulation is present under the roof. Our approach here is simple and analytical, to illustrate the significance of key parameters, especially the poorly-known convection coefficient. It is complementary to the work of Griggs et al. [14], who studied the sensitivity of roof temperature to various parameters numerically.

We will assume (for the purpose of this section) that thermal storage in the roof structure is not very important, as is the case for low mass construction. The main effects of thermal mass are to reduce and delay the daytime roof temperature peak, at the expense of heat release by the roof in the evening.

Subject to the above conditions, the heat balance on the roof surface can be written:

$$\alpha I = L_o + h_r(T_r - T_{air}) + h_c(T_r - T_{air}) \quad (1)$$

Here α is the solar absorptance, I is the solar insolation intercepted by the roof (maximum, about 1000 W m^{-2}), L_o is the thermal radiative cooling rate for roof temperature T_r equal to air temperature T_{air} (due to the radiant sky temperature depression below ambient air temperature), h_r is the radiative heat transfer coefficient, and h_c is the convection heat transfer coefficient. The radiative heat transfer coefficient h_r is readily computed from Planck's law if the spectral emittance of the roof is known. (Mathematically, one performs a Taylor's expansion in the parameter $(T_r - T_{air})$ and discards the small higher order terms.) If the emittance ϵ is independent of wavelength (gray body approximation), then $h_r = 4\epsilon\sigma T_{air}^3$, where σ is the Stefan–Boltzmann constant. For typical conditions of $\epsilon = 0.9$ and $T_{air} = 300$ K, the value of h_r is 5.5 W m^{-2} K^{-1}. The parameter L_o is proportional to ϵ and varies from about 50 to 100 W m^{-2} for blackbody ($\epsilon = 1$) horizontal surfaces exposed to clear skies, with the larger values associated with hot and dry conditions. It is reduced by cloud cover and is zero in fog. Thus it is usually small compared to the peak solar radiation flux but not negligible compared to the 24-h average solar flux. For more information on the estimation of thermal radiative cooling effects, see Ref. [15].

The convection coefficient h_c is usually the most difficult parameter in Eq. (1) to estimate. It is a sensitive function of windspeed, and also depends on the details of the roof roughness, height of the roof above ground level, and how the roof is exposed to the wind (presence of trees, etc.). In sunlight, with zero wind speed, h_c is determined by natural convection. It is a weakly increasing function of temperature difference

($\Delta T^{1/3}$), and almost independent of surface size in the turbulent regime of relevance here. For $T_r - T_{air} = 30$ K, standard engineering estimates [16] give $h_c = 6.6$ W m^{-2} K^{-1}, about the same as the radiative heat transfer coefficient. This reference gives the same value for horizontal and vertical surfaces (provided heat flow is upward). On the other hand, measured values for the windows of a 1 story building extrapolate at zero windspeed to 2.6 W m^{-2} K^{-1} [17]. These two values indicate the uncertainty in roof surface convection coefficients, often a factor of 2 or more, and also indicate that the zero wind speed (minimum) values of h_c are roughly half the size of h_r.

For wind speeds above about 1 m s^{-1}, the convection coefficient is determined by forced convection, and, for windows near the ground [17], rises from 2.6 at zero wind speed to about 18 W m^{-2} K^{-1} at speeds of 10 m s^{-1} (for upwind surfaces; lower values were found for downwind surfaces). (We are not aware of any comparable study for roof surfaces.) Reagan and Acklam made a few spot measurements of roof temperatures in Tucson [10]. They found rough agreement between measured and calculated roof temperatures using an algorithm which, for typical Tucson wind conditions, gave a coefficient in the range of 17 to 22 W m^{-2} K^{-1}. An explicit study of h_c for roof surfaces may in the future provide more accurate values. However, the values cited here are adequate to indicate roughly the magnitudes of the heat flows. Solving explicitly for the temperature difference in Eq. (1), we have

$$T_r - T_{air} = \frac{\alpha I - L_o}{h_r + h_c} \tag{2}$$

For peak solar heating conditions, L_o can be neglected unless α is very small. The peak temperature is then proportional to α and inversely proportional to the total heat loss coefficient $(h_r + h_c)$. Obviously, knowledge of the overall heat loss coefficient $(h_r + h_c)$ is just as important as knowledge of the solar absorptance α, for determining the temperature rise of the roof above ambient air temperature. For example, a ten percent error in α leads to a ten percent error in $(T_r - T_{air})$, which is acceptable in many applications. A ten percent error in $(h_r + h_c)$ also leads to an equivalent ten percent error in $(T_r - T_{air})$. However, knowledge of $(h_r + h_c)$ with an accuracy of ten percent is not feasible because of the large uncertainty in the convection coefficient h_c. Note that even sophisticated computer simulations of roof temperature also suffer from this same difficulty in estimating h_c. In contrast, if the roofing material has been optically characterized, then α and h_r are known, and measurements of $(T_r - T_{air})$ can be used to determine the convection coefficient h_c. Examples of this procedure will be given in Section 8.

3. Spectral reflectance measurements

Diffuse spectral reflectance in the spectral range of 0.3 to 2.5 μm was determined using a double-beam UV/VIS/NIR spectrophotometer (Perkin Elmer Lambda 9), fitted with a Labsphere RSA-PE-19 reflectance spectroscopy accessory (integrating sphere). The beam strikes the sample at nearly normal incidence (8° from the normal), and both diffuse and specular reflected radiation is collected by the integrating sphere. Reflectance was determined at wavelength intervals of 5 nm, relative to a Spectralon standard reflectance material (Labsphere). This standard reflectance material is a compacted polytetrafluoroethylene powder, which has been compared by the manufacturer to diffuse reflectance tiles calibrated by the National Institute of Standards (NIST). Our measurements of the spectral reflectance of another sample of Spectralon material agree well with values provided by the manufacturer, which shows the reproducibility of our measurement technique. However, it is necessary to rely on the calibration chain back to NIST for absolute values.

Spectral reflectances are converted to overall solar reflectances by weighted averaging, using a standard solar spectrum as the weighting function. The spectrum employed is that suggested by ASTM (see Standards E903 and E892), and represents both direct and diffuse solar radiation with the sun high in the sky. For opaque materials the reflectance is of course equal to $(1 - \alpha)$, where α is the solar absorptance introduced above.

4. Reflectance results

4.1. White paint

White acrylic paint (Fig. 1) is typical of a practical but high quality coating based on titanium dioxide (rutile) pigment in a transparent polymer binder. The strong absorption in the UV of the rutile pigment is regarded as a favorable feature because the absorption of the UV helps to protect the polymer and substrate. Pigment manufacturers optimize the particle size to obtain the highest possible reflectance in the visible range (centered in the green, at wavelength of

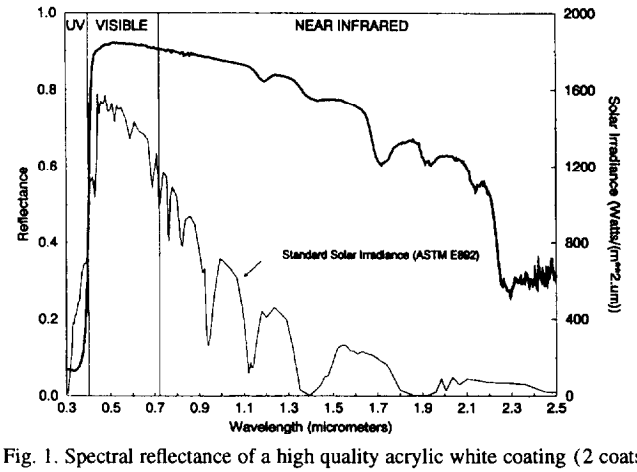

Fig. 1. Spectral reflectance of a high quality acrylic white coating (2 coats on a steel substrate). Also shown is the standard solar irradiance used as a weighting function for computing the overall solar reflectance (scale to right).

550 nm, or 0.55 μm). This optimum size is a particle diameter of about 200 nm. In this case the visible reflectance is over 90%. However the solar reflectance is only 83%. It could be raised by the use of larger particles, say 260 nm, which would improve the reflectance in the near-infrared. There are also some absorption features in the near-infrared, which are due to vibrations of hydrogen atoms in the coatings. Absorption due to heavier atoms occurs further out in the infrared (beyond 2500 nm). The strong (but unimportant) absorption near 2.3 μm is due to C–H bonds in the polymer. Some of the other absorption features, such as the dip at 1.7 μm, are also due to the polymer, but others are most likely due to hydrogen atoms in OH groups and H_2O. Manufacturers often coat rutile pigment for exterior use with metal hydroxide coatings, which can be one source of the OH absorption.

Also shown in the background of Fig. 1 is the ASTM standard solar irradiance distribution. This spectrum is provided in the background of some figures that follow, for the reader's reference. Solar reflectance data are presented in tables for three parts of the solar spectrum. The ultraviolet (UV) range extends from 300 to 400 nm, the visible range (VIS) from 400 to 720 nm, and the near-infrared (NIR) range from 720 to 2500 nm. Based on the standard spectrum the energy is distributed 5% UV, 46% visible, and 49% in the near-infrared. Note when a reflectance value is reported in the literature, sufficient details must be given so the reader can determine whether what is meant is the visible, solar, or some other reflectance. Here, of course, our primary interest is the solar reflectance.

4.2. White roof coatings

White roof coatings are excellent materials for reducing solar heat gain, as shown in Fig. 2. Tabulated values are collected in Table 1. Three coats were used on flat substrates. The solar reflectance is generally about 0.8. A comparison of the spectral curves shows that they are very similar, and are also similar to the artist' white shown in Fig. 1. The reflectance does fall off slowly in the infrared due to the use of pigment particle size optimized for high visible reflectance rather than high solar reflectance. Evidently all of these coatings use similar rutile pigments and polymers which are also similar. In addition to reducing air-conditioning energy use, these materials reduce the temperature excursions experienced by the roof. Since thermally-induced expansion and contraction can cause cracking, the use of white is an advantage. While the very highest reflectance is an advantage, the choice of a given coating in a given application may well be dictated by other considerations such as how well does the coating adhere? Does it remain flexible over time? Does it stand up to ultraviolet solar radiation and to moisture? Does dust adhere to it?

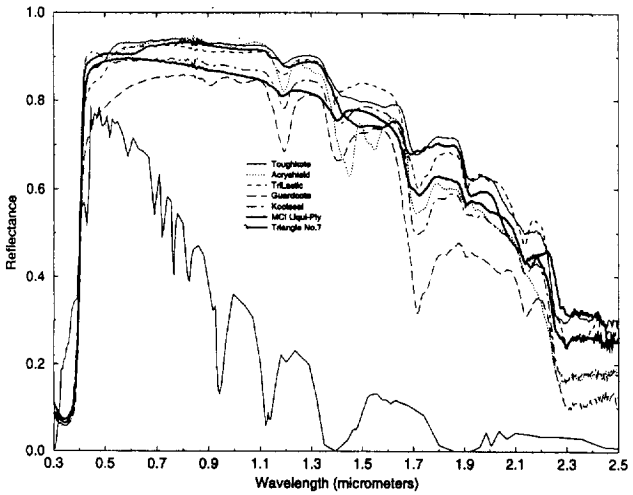

Fig. 2. Spectral reflectance of seven white roof coatings. Also, see Table 1.

Table 1
Reflectances for a group of commercial roof coatings, and an artist's white. Coating thickness varied from roughly 10 to 40 mils (0.25 to 1 mm) and substrates varied, so data cannot be used for precise comparison of the products listed. However, the performance of the coatings as a group is believed to be representative of new high quality white roof coatings applied to smooth substrates

Coating Reflectances	Solar	UV	VIS	NIR
Triangle Coatings, Toughkote	0.85	0.12	0.90	0.87
National Coatings, Acryshield	0.83	0.11	0.89	0.85
Triangle Coatings, Trilastic	0.83	0.11	0.88	0.86
Guardcoat	0.74	0.10	0.79	0.76
Koolseal elastomeric	0.81	0.14	0.88	0.81
MCI elastomeric	0.80	0.12	0.87	0.81
Triangle Coatings, high reflectance # 7	0.84	0.12	0.89	0.86
Utrecht acrylic artist's color, titanium white	0.83	0.16	0.90	0.83

4.3. White roof membranes

We tested four white single-ply polymeric roof membranes. Unlike a roof coating, which is applied to a roof membrane surface for protection, single-ply roof membranes are designed to serve as complete roofing systems. They are typically prefabricated into flexible sheeting that is either ballasted with gravel or attached at the surface. Spectral reflectance data for such roofing membranes are shown in Fig. 3 and Table 2. The solar reflectances are, like the white coatings, generally about 0.8. Obviously, ballasting with gravel would reduce this high value.

4.4. Aluminum pigmented roof coatings

Fig. 4 shows the spectral reflectance data for several aluminum roof coatings on various substrates. These materials consist of aluminum metal pigment flakes in a black asphalt-type binder. The trend of reflectance increasing with increasing wavelength, and the dip at 0.8 μm, are both characteristics of pure aluminum. Unlike white coatings, which absorb the ultraviolet (below 0.4 μm), the aluminum coatings are more reflective in this range. While each coating is qualitatively similar to the others, the overall solar reflectance ranges from 30 to 56%. We surmise that the variation in reflectance is due

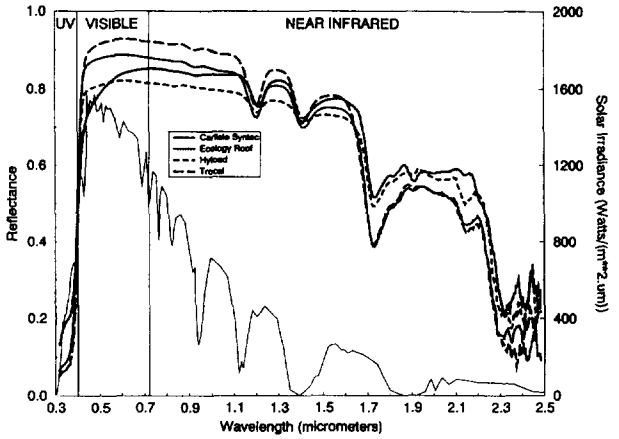

Fig. 3. Spectral reflectance of some white roofing membranes. Also, see Table 2.

Table 2
Solar reflectance for some single-ply roofing membranes

White polymer membrane reflectances	Solar	UV	VIS	NIR
Carlisle Syntec Systems Brite-ply	0.77	0.25	0.80	0.79
Ecology Roof	0.80	0.19	0.87	0.79
Hypsam Roofing Systems Hyload	0.75	0.16	0.81	0.75
Trocal Roofing Systems white	0.83	0.14	0.91	0.82

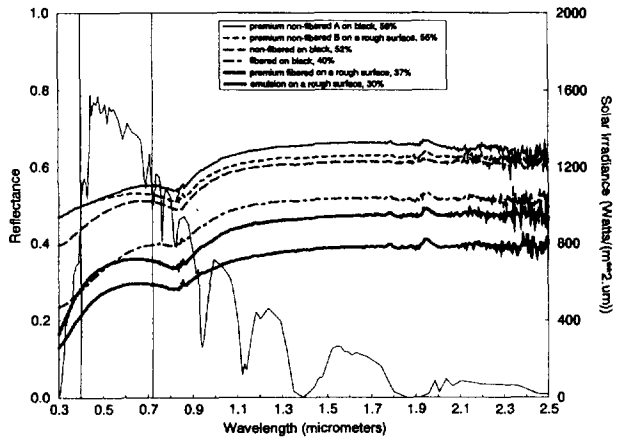

Fig. 4. Spectral reflectance of several aluminum pigmented roof coatings. Overall solar reflectances are listed in the inset.

to the varying fraction of the aluminum which is exposed at the coating surface.

Most building materials have an infrared emittance of about 0.9, but metals usually have a lower emittance. Measured values of ϵ are desirable, because the eye is completely insensitive in the 5 to 40 μm wavelength range of importance: transparent coatings on the surface of a metal can greatly change the emittance without altering its visual appearance. We measured the emittance with a portable, ambient temperature emissometer (Model 2158, International Technology Corp., Satellite Beach, FL). This technique uses a vacuum thermocouple inside a heated sensor head to monitor the effect of emittance on radiant heat flow. The samples were placed on a metal plate which serves to stabilize their temperatures, along with reference standards which were 3M

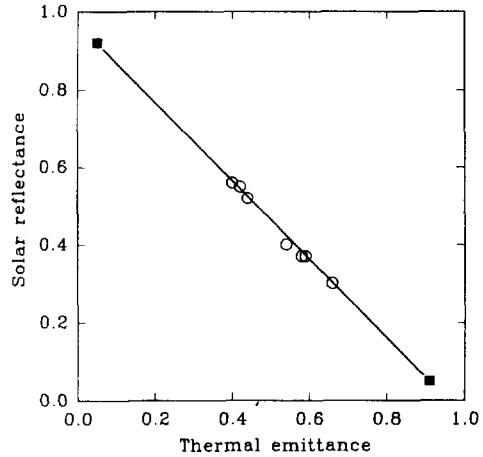

Fig. 5. Correlation between the solar reflectance and thermal emittance of aluminum roof coatings. End points are based on estimated values for bare aluminum and asphalt.

Nextel black paint ($\epsilon \cong 0.96$) and a clean aluminum surface ($\epsilon \cong 0.06$). The sensor head was then placed on the samples, and the emittance was determined by interpolation using the standards as references.

The emittance results, which are accurate to roughly ± 0.05, are plotted together with solar reflectance values in Fig. 5. Note that there is a correlation between the two quantities. Presumably, the fraction of exposed aluminum determines where a given sample falls on the line. Consider also the thermal reflectance, that is, the average reflectance in the 5 to 40 μm wavelength range. It is equal to $(1-\epsilon)$ for these opaque samples. We can see that the thermal reflectance is nearly equal to the solar reflectance, but that the thermal reflectance is consistently slightly larger. This higher reflectance at longer wavelengths is consistent with a continuation of the trend in Fig. 4, namely that reflectance increases with wavelength.

Fig. 5 shows that there is a trade-off for aluminum-filled cool roof coatings. Higher solar reflectances are achieved with more exposed aluminum flake, but this is offset by the lower emittance observed in our correlation. If convection was not important, a reflective aluminum surface could become even hotter in the sun than a black but emissive material. However, because convection is usually at least as important as cooling by infrared emission ($h_c \geq h_r$), there is generally a significant advantage in the use of aluminum coatings in place of dark colors.

4.5. Asphalt shingles

The spectral reflectances of a number of asphalt shingles is shown in Fig. 6 and Table 3. Note that even the typical 'white' asphalt shingle has a low solar reflectance of 21%. (Other typical white asphalt shingles we have measured fall in the range of 21 to 29%; premium white shingles are a bit higher.) These materials are manufactured by pressing coated rock granules into the asphalt. The granules have been fabricated by the crushing of rock (e.g., granite) followed by

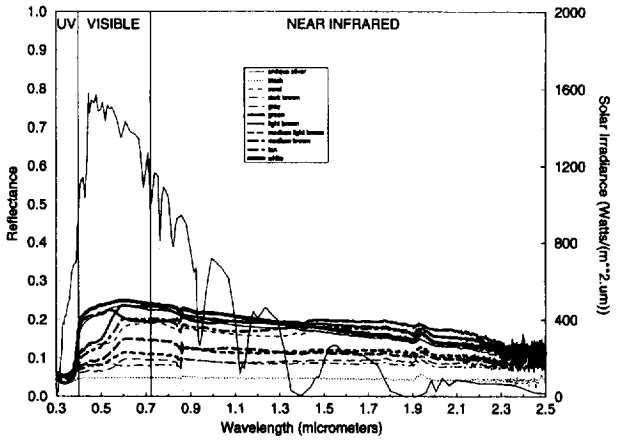

Fig. 6. Spectral reflectance of several asphalt roofing shingles. The discontinuity at 0.86 μm and the bump at 1.93 μm are artifacts of the data collection process due, in part, to sample roughness. They however do not significantly affect the overall solar reflectance.

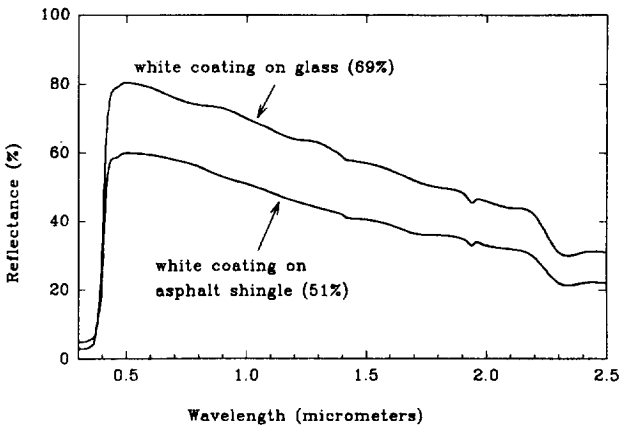

Fig. 7. Spectral reflectance of the same white coating applied to a smooth glass substrate, and on a rough asphalt shingle. The asphalt shingle is covered with granules, each about 1 mm in diameter.

Table 3
Reflectance of asphalt shingles

Asphalt shingle reflectances	Solar	UV	VIS	NIR
Antique silver	0.20	0.06	0.22	0.19
Black	0.05	0.04	0.05	0.05
Coral	0.16	0.05	0.16	0.17
Dark Brown	0.08	0.05	0.08	0.09
Gray	0.08	0.06	0.08	0.09
Green	0.19	0.08	0.21	0.20
Light Brown	0.19	0.07	0.19	0.20
Medium Light Brown	0.10	0.05	0.10	0.11
Medium Brown	0.12	0.06	0.12	0.12
Saddle Tan	0.16	0.05	0.16	0.18
White	0.21	0.06	0.24	0.21

application of an inorganic coating which contains pigments which are quite similar to those used to color paint. While it has been fairly well known that conventional asphalt shingles have low solar reflectances [10,11], it has been less clear why the values are so low. For a white shingle, for example, several factors must contribute to the low reflectance relative to a white paint coating with reflectance of 0.8. These are incomplete coverage (asphalt substrate shows through), lower reflectance of the coating (due to use of less pigment, impurities in pigment, or thinner coating), and the effects of roughness. The effects of roughness will be discussed in the next section. Evidently, each of these three factors contributes to the low reflectance.

5. Effects of roughness

As is well known, roughness lowers the reflectance of a surface. A smooth white coating is actually rough on the scale of the wavelength of light; that is why it appears white rather than glossy or mirror-like. However, it is the roughness on size scales larger than the wavelength of light which concerns us here. The reflectance is the probability that an incident photon is reflected when it encounters a surface. If the surface in question is rough rather than smooth, a photon which is reflected once is likely to require one or more additional reflections before it escapes. Thus the probability of absorption is increased.

To estimate the importance of roughness for asphalt shingles, we sprayed a white aerosol coating (2 coats) on a typical white shingle and on a microscope slide. The exposed surface area of the shingle was estimated to be about twice its nominal area. The coating thickness was about the same in both cases, as was judged by weighing the samples. The measured spectral reflectances are shown in Fig. 7. The spectral shapes of the curves are very similar, but the rougher surface has only about 3/4 of the reflectance of the smooth surface. Stated in terms of the absorptance α one can see that absorptive materials, as these coatings are in the ultraviolet range, are even darker when roughened, but the absorptance is little changed and is already close to unity. However, a reflective material, as these coatings are in the visible at 0.5 μm, is greatly affected by roughness. The visible absorptance of 20% for this white coating is increased to 40% by the roughness of the shingle. Thus, it is clear that the roughness of asphalt shingles contributes significantly to their generally low reflectance.

The impact of roughness on solar absorptance also complicates the estimates of reflectance for metal roofing materials which are corrugated to provide stiffness. A white coating on a metal roofing panel may have a reflectance of 0.7 as measured in the laboratory on a small sample. But the corrugation will reduce the reflectance, and furthermore, will reduce it by an amount which depends on the angle of the incident radiation. Numerical calculations for a few simple shapes would be helpful to clarify this problem. Oren and Nayar [18] have recently developed a model of rough surfaces which may be helpful in evaluating the effects of surface roughness in more detail.

6. Effects of purity

Many highly reflective materials consist of pigment particles which scatter light effectively, suspended in a transparent matrix. White paint is an example. Photons of light incident on such a coating tend to be scattered many times before emerging from the coating as reflected light. Due to this 'random walk' of the photons in scattering media, the path the reflected photon must traverse can be rather long, and small quantities of absorbing materials can reduce the reflectance dramatically. Bohren discusses this sensitivity of multiple scattering media to small amounts of absorption [19].

One good example of how the purity of a material can adversely affect its reflectance is given by the work of Morris et al. [20]. They were interested in the solar spectral reflectance of the surface of Mars, and investigated hematite pigments. These iron oxide (Fe_2O_3) pigments are often used in red materials here on earth; the same compound is also responsible for the color of red clay and red concrete roofing tiles. The pigment in question contained a small amount of magnetite, another iron oxide (Fe_3O_4). Magnetite is a black pigment. The presence of a small amount of magnetite made only a slight difference in the visible color of the pigment, but greatly reduced the reflectance in the infrared, especially between 1.1 and 2.1 μm wavelength. This fact was demonstrated by heating the contaminated pigment in air, oxidizing the compound Fe_3O_4 to Fe_2O_3. After heating, the reflectance in the 1.1 to 2.1 μm range was raised from 0.2 to 0.8.

7. Other reflective materials

Several novel materials were prepared for analysis, which might be cooler than materials presently used. Since white materials already exhibit fairly good performance, we examined black, green, and red materials. To avoid any possible misunderstanding, we emphasize that these novel materials are not commercial building materials.

For the black, we took a black paint, and covered it with a stick-on window coating (coated polymer film) which transmits visible light but reflects infrared radiation. The reflectance spectrum is shown in Fig. 8. The film did increase the visible reflectance slightly, adding some specular reflectance, but the sample still appeared black. The solar reflectance was increased from 5% to 33%, a considerable gain. The infrared emittance was reduced and had a complex spectral structure due to the thin films used to produce the high near-infrared reflectance. While this example shows conceptually that the solar reflectance can be increased without much change in the visible reflectance, cost and durability considerations presently preclude its consideration as a roofing material.

The reflectance of three green materials, with Cr_2O_3 pigment, is shown in Fig. 9. As is well known, chromium oxide pigment has a high infrared reflectance [21]. The green asphalt shingle, reflecting only 14%, is surpassed by the dark green Cr_2O_3 pigmented film (24%), and the light green film

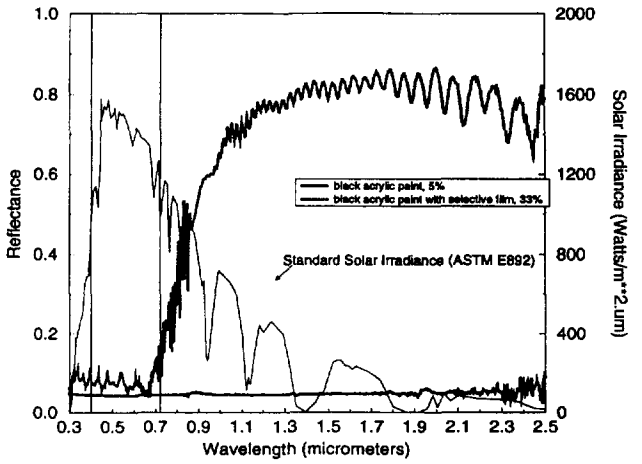

Fig. 8. Spectral reflectance of a black acrylic paint and the same paint covered with a selective infrared-reflective window film. This is a polymer film used to reflect infrared radiation while admitting visible light. This film is 60% transparent in the visible spectrum (30% absorption, 10% reflection), and rather reflective in the infrared, as is apparent.

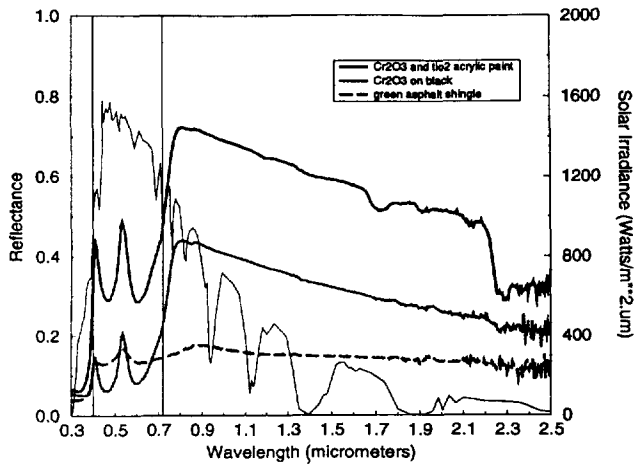

Fig. 9. Spectral reflectance of three green materials with chromium oxide pigment. These materials appear green due to the peak in the reflectance spectrum at 0.5 μm.

with added TiO_2 (48%). This example, and the next, show that films do not have to be white to have solar reflectances of the order of 50%. It seems likely that, with optimized (possibly larger) particle size, the infrared reflectance of the Cr_2O_3 coatings could be further increased.

Four red materials, with hematite pigments, are shown in Fig. 10. The highest reflectance (43%) was achieved with a light red color, using both Fe_2O_3 and TiO_2. The pure hematite pigment in an acrylic binder achieved a reflectance of 25%, applied over a black substrate. A red clay tile displayed an even higher reflectance, 33%. (Parker et al. [11] measured a red concrete tile at 18%.) Note that the reflectance of the clay tile exceeds 50% in most of the infrared spectrum. A coral (red) asphalt shingle is included for comparison; its solar reflectance is about 14%.

8. Temperature measurements in sunlight

In support of the optical measurements reported above, we made simple outdoor temperature measurements on two

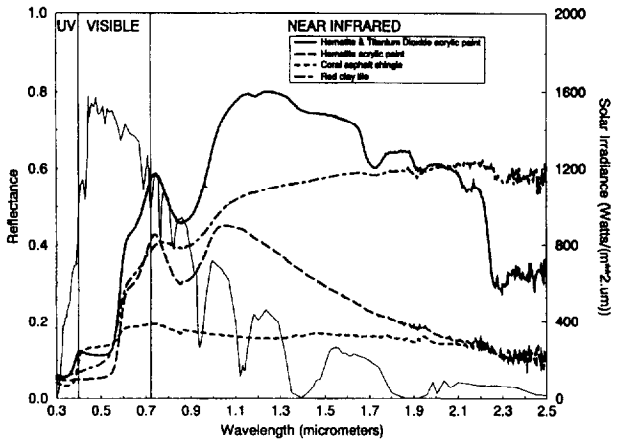

Fig. 10. Spectral reflectance of four red materials with hematite pigment. The increase in reflectance at 0.58 μm makes these materials appear red. The dip near 0.9 μm is also characteristic of the hematite material.

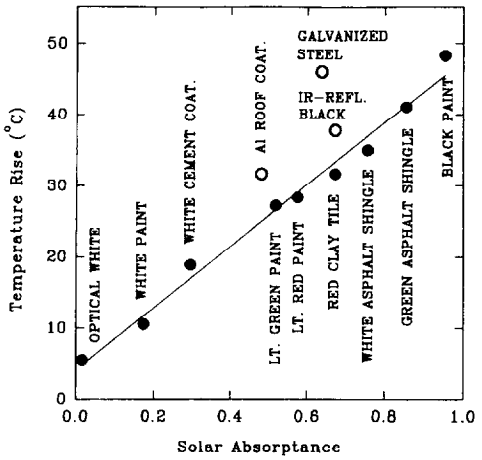

Fig. 11. Temperature rise above air temperature for twelve samples exposed to full sunlight on an insulated substrate. The filled circles are samples with emittances of about 0.9, and the open circles are samples with lower infrared emittances. The straight line is a fit to the data through the filled circles. Samples are described in the text.

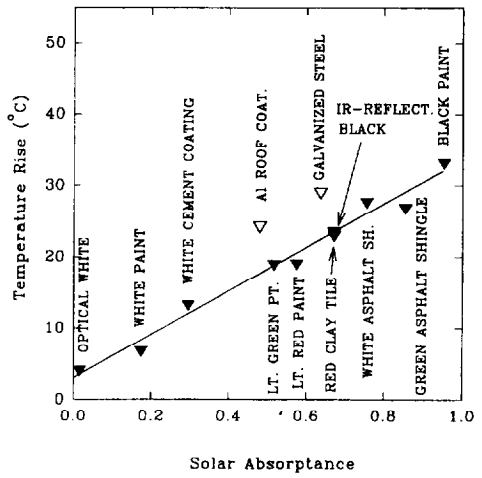

Fig. 12. Data as in Fig. 8, but for a day in July rather than in November. One open triangle is partly covered by a solid triangle.

occasions on the roof of a four-story building at our Berkeley laboratory. Twelve 10 cm square samples in a 3 by 4 array were attached to an insulating foam board which had been covered with an unpainted cotton artist's canvas. Underneath each sample was a thermocouple for monitoring the sample temperature. The presence of the insulating foam substrate, and secure sample mounting with double sided tape, ensured that the thermocouples accurately measured the sample temperatures. For the November experiment, the sample board was placed on a wooden roof platform only 10 cm above the roof surface, and tilted up to face the midday sun (zenith angle, 55°). For the July experiment, the sample board was placed on a small table, 75 cm high, and tilted to face the midday sun (zenith angle, 15°). No on-site wind measurements were performed. However, the wind conditions were qualitatively similar on both days: breezy enough to move papers around but less than a stiff wind. The detailed wind conditions and the details of sample exposure no doubt affect the effective convection coefficient.

The effects of convection are quite evident in such an experiment. Each sample attains its maximum, or stagnation, temperature after a few minutes in the sun. Thereafter, the sample temperatures fluctuate erratically, by several degrees, as gusts of wind come and go. These temperature fluctuations are caused by the time varying convection coefficient, and are moderated but not eliminated by the heat capacities of the samples. The results of the November measurement are shown in Fig. 11, as a function of solar absorptance. The temperature rise plotted here is measured relative to the local air temperature. The filled circles are all materials with infrared emittance of about 0.9. From left to right they are an optical white (Spectralon, see Section 3), white acrylic paint, white cementitious coating, green acrylic paint (with TiO_2), red acrylic paint (with TiO_2), a red clay tile, white asphalt shingle, green asphalt shingle, and black acrylic paint. The straight line is a fit through the filled circles. From left to right, the open circles, samples with emittance significantly below 0.9, are an aluminum pigmented asphalt coating, clean galvanized steel, and infrared-reflective film on black. Note that the temperature of the $\epsilon = 0.9$ samples is well correlated with the solar absorptance measured in the laboratory, particularly considering the limited precision of the temperature measurements due to fluctuations. The samples with lower emittance fall above the fitted line due to their reduced ability to radiate heat by infrared radiation. Galvanized steel is particularly poor, as its solar absorptance is above 0.6 and its infrared emittance is roughly 0.1: it is nearly as hot as black.

Fig. 12 shows data analogous to those of Fig. 11, but for a day in July. In this case the temperature rise of the samples was smaller than those of the November day, but the results are otherwise quite similar. Again, there is a good correlation of temperature rise with solar absorptance.

An approximate convection coefficient for these outdoor measurements can be inferred from the slope of the lines in Figs. 11 and 12. According to Eq. (2), this slope is $I/(h_r + h_c)$. Using a nominal value of 1000 W m^{-2} for I and 5.5 W m^{-2} for h_r, we find that the convection coefficient h_c is roughly 18 W m^{-2} K^{-1} for Fig. 11 and 25 W m^{-2} K^{-1}

for Fig. 12. The larger value for h_c, for the July data, may be either due to windier conditions or the fact that the experimental board was attached higher above the roof.

Another interesting aspect of the data in Figs. 11 and 12 is that the intercepts of the plots occur at a positive temperature, about 4°C above air temperature. This is not what is expected from Eq. (2) with zero solar gain. The intercept should be negative, about −2°C. Also, it is readily observed that early and late in the day, when the samples are not intercepting full sun, that the white samples cool below air temperature. Thus the expected radiative cooling effects are indeed present. The best explanation found to date for the positive intercept is that there is a significant edge effect with these small 10 cm square samples. Infrared thermography was used to examine the temperature distribution of the samples and their surrounding background, the canvas-covered foam insulation. It revealed that the sample temperatures were rather uniform, but that temperature gradients were present around those samples which were warmer or cooler than the background. The background was at about the same temperature as the white cementitious coating. Thus, edge-effect heat conduction causes the cooler samples to be warmed by their surroundings and the hotter samples to be cooled. It is difficult to provide quantitative estimates of the magnitude of the edge effect. Some of this effect is due to heat transfer from sample to background by means of convection in the air above the samples. Allowance for it would have the effect of making the slope of the lines in Figs. 11 and 12 steeper, reducing the y-axis intercept toward negative values, and reducing the value given by our spot measurements of h_c. In the future, this type of edge effect can be reduced by the use of larger samples, and by the use of 'background' materials which are close in optical properties to the samples under test.

9. Conclusions

We have characterized the solar reflectance of a number of roofing materials with spectral reflectance measurements, and discussed how the reflectance depends upon the materials chosen, the surface roughness, and the presence of impurities. For aluminum roof coatings, a correlation between solar reflectance and thermal emittance was presented. Brief outdoor measurements demonstrate the expected strong correlation between solar reflectance and surface temperature in sunlight. For keeping surfaces cool, one wishes to have large values for the solar reflectance, thermal emittance and convection coefficient.

More data on the solar reflectance of practical building materials are still needed, to supplement the sketchy literature. For example, additional data are needed on different types of concrete, coated metal roofing materials, roofing tiles, etc. At present it is not possible to estimate reflectance of gravel-ballasted roofs based on laboratory reflectance measurements. In this case on-site pyranometer measurements would be helpful to document the solar reflectance of the different materials.

Acknowledgements

We have benefited from conversations with Hashem Akbari, Arthur Rosenfeld, and Danny Parker. Brent Griffith arranged for the real-time thermography. M. Sharfstein of Southwall Technologies supplied the infrared-reflective window film. This work was supported by the US Department of Energy under contract DE-AC03-76SF00098.

References

[1] D.S. Parker, J.B. Cummings, J.S. Sherwin, T.C. Stedman and J.E.R. McIlvaine, Measured air-conditioning electricity savings from reflective roof coatings applied to Florida residences, *Rep. No. FSEC-CR-596-93*, Florida Solar Energy Center, 300 State Rd. 401, Cape Canaveral, FL 32920, 1993.

[2] C. Boutwell, Jr., Y. Salinas, P.R. Graham, J.A. Lombardo and L. Rothenberger, *Building for the Future, Phase I*, Vol. I, Dept. of Construction and Architectural Engineering Technology, University of Southern Mississippi, 1986.

[3] H. Akbari, S. Bretz, D.M. Kurn and J. Hanford, Peak power and cooling energy savings of high-albedo roofs, submitted to *Energy and Buildings*. See also, H. Akbari, S.E. Bretz, J.W. Hanford, D.M. Kurn, B.L. Fishman, H.G. Taha and W. Bos, Monitoring peak power and cooling energy savings of shade trees and white surfaces in the Sacramento municipal utility district (Smud) service area: data analysis, simulations, and results, *Rep. No. LBL-34411*, Lawrence Berkeley National Laboratory, Berkeley, CA, 1992.

[4] S.L. Baron (ed.), *Manual of Energy Saving in Existing Buildings and Plants, Facility Modifications*, Vol. II, Prentice-Hall, Englewood Cliffs, NJ, 1978, pp. 123–125.

[5] C.W. Griffin, Cost savings with heat-reflective roof coatings, *Plant Engineering*, July 10 (1980) 98.

[6] D.W. Yarbrough and R.W. Anderson, Use of radiation control coatings to reduce building air-conditioning loads, *Energy Sources, 15* (1993) 59.

[7] E.I. Griggs and P.H. Shipp, The impact of surface reflectance on the thermal performance of roofs: an experimental study, *ASHRAE Trans., 94* (1988) 1626. See also *ARHRAE Handbook of Fundamentals*.

[8] J.D.N. Nisson (ed.), Clay tiles for cool roofs, *Energy Design Update 11*, Cutter Information Corp., Arlington, MA, 1992.

[9] H. Taha, D. Sailor and H. Akbari, High-albedo materials for reducing building cooling energy use, *Rep. No. LBL-31721*, Lawrence Berkeley National Laboratory, Berkeley, CA, 1992.

[10] J.A. Reagen and D.M. Acklam, Solar reflectivity of common building materials and its influences on the roof heat gain of typical southwestern US residences, *Energy Build., 2* (1979) 237.

[11] D.S. Parker, J.E.R. McIlvaine, S.F. Barkaszi and D.J. Beal, Laboratory testing of reflectance properties of roofing materials, *Rep. No. FSEC-CR-670-93*, Florida Solar Energy Center, 300 State Rd. 401, Cape Canaveral, FL 32920, 1993.

[12] Y.S. Touloukian, D.P. DeWitt and R.S. Hernicz, *Thermal Radiative Properties, Coatings, Thermophysical Properties of Matter*, Vol. 9, IFI/Plenum, New York, 1972.

[13] R. Furler, P. Williams and F.K. Kneubuhl, Survey on spectral infrared and optical properties of building glasses and panes, *Infrared Phys., 33* (1992) 321.

[14] E.I. Griggs, T.R. Sharp and J.M. MacDonald, Guide for estimating differences in building heating and cooling energy due to changes in solar reflectance of a low-sloped roof, *Rep. No. ORNL-6527*, Oak Ridge National Laboratory, Oak Ridge, TN, 1989, pp. 1–57.

[15] P. Berdahl, M. Martin and F. Sakkal, Thermal performance of radiative cooling panels, *Int. J. Heat Mass Transfer, 26* (1982) 871; M. Martin and P. Berdahl, Summary of results from the spectral and angular sky radiation measurement program, *Solar Energy, 33* (1984) 241; M. Martin and P. Berdahl, Characteristics of infrared sky radiation in the US, *Solar Energy, 33* (1984) 321.

[16] F. Kreith and M.S. Bohn, *Principles of Heat Transfer*, Harper Collins, New York, 1986, Eqs. (5.13) and (5.16b). See also *1989 ASRAE Handbook, Fundamentals*, American Society of Heating, Refrigerating, and Air-Conditioning Engineers, Atlanta, GA 30329, 1989, p. 3.12.

[17] M. Yazdanian and J.H. Klems, Measurement of the exterior convective film coefficient for windows in low-rise buildings, *ASHRAE Trans., 100* (1994) 1087.

[18] M. Oren and S.K. Nayar, Generalization of the Lambertian model and implications for machine vision, *Int. J. Computer Vision, 14* (1995) 227.

[19] C.F. Bohren, Multiple Scattering of light and some of its observable consequences, *Am. J. Phys., 55* (1986) 524.

[20] R.V. Morris, H.V. Lauer, Jr., C.A. Lawson, E.K. Gibson, Jr., G.A. Nace and C. Stewart, *J. Geophys. Res., 90* (1985) 3126.

[21] D. Stevens, Chromic oxide green, in P.A. Lewis (ed.), *Pigment Handbook, Properties and Economics*, Vol. 1, Wiley, New York, 2nd edn., 1988, pp. 311–313.